Hindawi
Shock and Vibration
Volume 2023, Article ID 2859668, 10 pages
https://doi.org/10.1155/2023/2859668

Research Article

Study on Muck Pile Shape of Open-Pit Bench Blasting Based on PFC

Wenle Gao,[1] Jianwei Zhang,[1] Chenhao Li,[1] Lin Cheng,[1] and Penghui Liu[2]

[1]*College of Civil Engineering and Architecture, Shandong University of Science and Technology, Qingdao 266590, China*
[2]*Qingdao Public Architecture Design Institute Co., Ltd., Qingdao 266071, China*

Correspondence should be addressed to Jianwei Zhang; jianweizhang1017@163.com

Received 21 February 2023; Revised 23 May 2023; Accepted 2 June 2023; Published 17 June 2023

Academic Editor: Lei Weng

To study the influence of different resistance lines and rows delay intervals on the shape of the muck pile and the throwing distance of open-pit bench blasting based on the open-pit bench blasting test, two-dimensional particle flow code (PFC2D) is used for numerical simulation. The experimental and simulation data were compared and analyzed, and the error value was acceptable. Meanwhile, different resistance lines and row delay intervals are used to conduct numerical simulation analysis. The results show that the height change of the muck pile is directly proportional to the resistance line, and the rock throwing distance is inversely proportional to the resistance line change. The best resistance line is 1.75 m in the actual working condition, according to the effect of the muck pile. By fitting the relationship between the resistance line and rock throwing distance and blasting muck pile's height, it is found that the relationship is nonlinear. By simulating different row delays, the optimal row delay time difference in the bench blasting model is determined to be 25 ms under similar working conditions. It provides a guiding significance for the blasting parameter design under similar working conditions.

1. Introduction

Current numerical simulation is mainly divided into the finite element method based on continuum mechanics and the discrete element method based on Newton's classical mechanics [1]. The simulation of rock blasting research mainly adopts the finite element method, and the rock is regarded as a continuum medium [2]. Comparatively speaking, the discrete element method has excellent advantages in predicting rock motion and the blasting effect during blasting.

An et al. [3, 4] proposed a hybrid finite-discrete element method to simulate the dynamic fracture, fragmentation, and muck pile formation in blasting mining and calibrated the FDEM by simulating the process of blasting crater formation. It is found that FDEM can reasonably simulate the stress and fracture propagation process and the formation process. The mixed finite element and discrete element method is used to simulate the process of rock breaking and throwing and the formation of muck piles caused by blasting under different conditions. Various factors affecting explosive rock breaking are studied. Prasad et al. [5] studied the influence of blasting design parameters on rock fragments by conducting tests and determining the rock fragment size and maximum fragment size using computer software. It is found that the length of blast hole plugging and charge consumption greatly influence rock fragmentation. Hudaverdi and Akyildiz [6] proposed a new classification method for predicting blasting flying rock throwing distance based on field measurement and conducted multiple regression analyses on blasting data to establish a prediction formula for blasting flying rock. Yu et al. [7] used the simulation method composed of the finite element simulation of explosion load calculation and bonded particle method simulation of bench blasting to study the rock movement caused by blasting. They verified the simulation results through theoretical analysis and field monitoring. Yan et al. [8] established a new method based on the 3DEC program to simulate the cracking and throwing process of blasting funnel and bench blasting considering

the rock fragmentation size. It is found that the discretized simulation of the bench blasting profile considering the degree of rock fragmentation is consistent with the prediction results of the traditional ballistics theory and that the maximum casting distance and muck pile height obtained by the two methods have little difference. Su et al. [9] used discrete element PFC2D software to study the relationship between blasting parameters and the shape of the muck pile. The research results show that the throwing distance is directly proportional to the height of the bench and inversely proportional to the size of the resistance line. The relationship between the muck pile height and blasting parameters is opposite to the throwing distance. Procházka [10] proposed a discrete hexagonal element method instead of the method to solve the persistent problem and analyzed the generation of the rockburst problem. Zhou et al. [11] compared the difference between the particle flow and other simulation methods. They used the particle flow method to simulate biaxial, Brazilian splitting, chamber excavation, and rock caving. Yang et al. [12] adopted the particle flow method to simulate the explosion of the cylindrical charge and the damage process of the rock mass. The authors established the explosion particle expansion loading method and the dynamic boundary treatment method according to the discrete element mechanism and compared the blasting funnel action index with the field test results to verify the rationality of the numerical model of cylindrical charge explosion. Ma et al. [13] established the numerical model of blasting rock breakage and throwing based on the field experimental data and blasting theory and studied the influence of blasting parameters on the effect of rock throwing. It is found that the single consumption of explosives and the hole distance have the most significant influence on the throwing effect of rock, and the calculation formula of the limit value of the single consumption of explosives and the hole distance is obtained. The mechanism and mechanical behavior of deep bench blasting throwing are revealed.

There are a lot of joints and fissures in the rock. The rock in the region is divided into rock blocks of different sizes, and the interior of the rock blocks can be regarded as a continuum medium. Nevertheless, the rock mass in the whole region should be studied as a discontinuous medium due to its internal structural plane. However, the particle discrete element method cannot be limited by the size of rock deformation. It can better simulate rock media cracking, separation, cracks, and other discontinuous changes [14]. In this work, the simulation of open-pit bench blasting used particle flow software PFC5.0 and the blasting effect is optimized from two aspects of row delay and resistance line [15, 16]. It has a specific guiding significance for blasting engineering with similar working conditions.

2. Particle Flow Discrete Element Theory

2.1. Applying the Blasting Load. The grain flow discrete element program in PFC cannot directly define particles of explosive material, giving relevant explosion material properties to simulate the dynamic process. The particle expansion exerts the load method for the explosive load, and the simulation results are closer to reality.

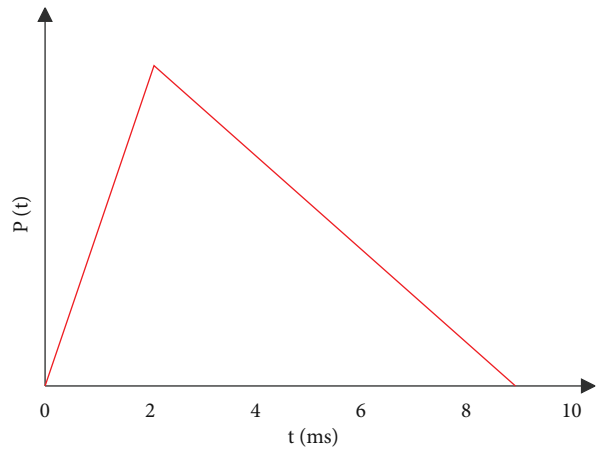

Figure 1: Schematic diagram of explosion stress wave.

Due to the explosion site's complexity and danger, the explosion load's active form still relies on some empirical formulas. In the existing studies, the application of the explosion load usually adopts the triangular distributed load model. It can well reflect the fluctuation characteristics of the outgoing load, as shown in Figure 1. Therefore, the explosion process can be simulated by applying the corresponding stress wave to the borehole wall.

2.2. Boundary Conditions. There are two commonly used methods to simulate the boundary of the infinite medium rock mass: one is the viscous boundary and the other is the transmission boundary method. The transmission boundary method will cause the particle velocity in the boundary range to be almost zero, and the stress wave will not propagate to the boundary, which directly leads to the sudden drop of the peak value of the stress wave near the boundary. Nevertheless, this differs from the field's stress wave propagation law. Therefore, the viscous boundary method is closer to reality, and the simulation of an infinite medium uses the viscous boundary.

In the particle flow method, the boundary force is applied to the boundary particles near the wall to offset the transmitted stress wave and prevent the reflected stress wave from accumulating stress inside the model. The relationship between the boundary force and the particle movement velocity is as follows:

$$F = -2R\rho Cu. \tag{1}$$

R is the radius of suspended particles, ρ is the rock density, C is the stress wave velocity, and u is the particle velocity.

If incident vibration wave U exists at the boundary, the contact force between particles can be written as follows:

$$F = 2R\rho C[2U - u]. \tag{2}$$

Table 1: Physical and mechanical test parameters of limestone.

Parameters	Uniaxial compressive strength (MPa)	Density (kg/m^3)	Poisson ratio	Elastic modulus (GPa)	Angle of internal friction (°)
Average value	81.2	2720	0.23	65	30

Blasting stress waves propagates in the medium, resulting in a dispersion effect and attenuation of stress wave intensity. Therefore, the above formula must be modified to obtain more accurate results:

$$F = \begin{cases} -\alpha \bullet 2R\rho C_p u_n, \\ -u \bullet 2R\rho C_s u_s. \end{cases} \quad (3)$$

3. Parameter Calibration of the Particle Flow Discrete Element Rock Mass Model

The test mining area is located on the Zaozhuang fault's north wall, and the mine's lithology is mainly medium-thick limestone. The representative rock blocks with relatively intact rocks and no obvious cracks on the surface are selected from the limestone stones in the mining area for core drilling and sampling. The standard rock sample with a diameter of 50 mm and a height of 100 mm was selected for the rock uniaxial compression tests, and the mechanical parameter statistics of the rock sample are shown in Table 1 [17].

The microparameters of the model were calibrated based on the macroscopic mechanical parameters obtained from the uniaxial compression experiment. The particle discrete element model of microparameters mainly includes the model outline of parameters and the model of contact between particles. Among them, the contact parameter between particles is the main influencing parameter affecting the intensity of the model.

To match the parameters of the subsequent bench blasting model, the uniaxial compression test model and the bench blasting test model adopted the same particle radius range and generation mode. A plane 2D particle discrete element uniaxial compression model is established with an aspect ratio of 2 : 1, a width of 50 mm, and a height of 100 mm [18, 19]. To prevent particles from escaping from the wall during loading, the stiffness of the loaded wall should be much higher than particle stiffness, usually set to 10~15 times the wall stiffness [20].

The simulated curve is close to the test curve, and the error is within an acceptable range. According to the calibration law, certain microparameters can be fine-tuned to make their fitting degree higher because it has little influence on the determined curve. The stress-strain curves obtained by calibration and those obtained by the laboratory test are shown in Figure 2. It can be seen from the figure that the calibrated curves obtained by adjusting each microparameters are consistent with those obtained by the uniaxial compression test. Although the slope of the simulated curve is slightly smaller than that of the test curve, the error is only 3.65%, which is within the acceptable range [21]. The peak stress of the simulated curve is slightly larger than that

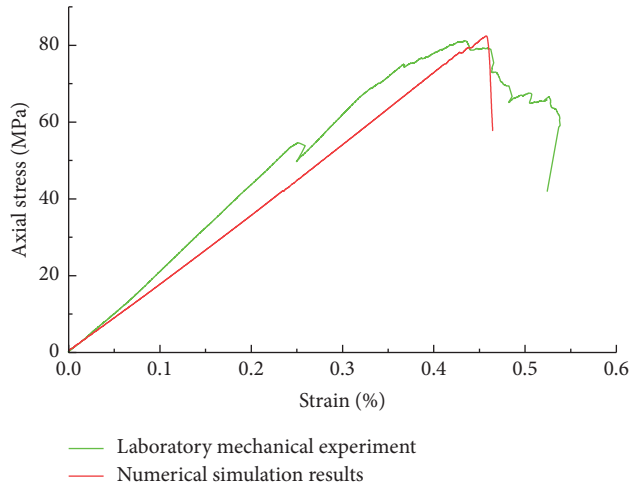

Figure 2: Comparison of microparameters calibration curves.

of the experimental value, with an error of 1.48%. The fitting degree of peak stress is higher than that of elastic modulus. Therefore, the obtained microparameters can be used to establish the bench model. The microparameters of the model are shown in Table 2.

4. Numerical Simulation

The particle flow discrete element model was established according to the size of the explosion zone, bench height, and blasting parameters. The model adopted the parallel bonding model with a length of 60 m and a height of 22 m, as shown in Figure 3. The bench height is 11 m, there are four rows of holes in total, the hole distance is 4.4 m, and the depth of the holes is 13 m. The length of the blocking section is 3 m. The blast hole used a cylindrical charge. According to the Starfield superposition principle [22], the superposition of the spherical charge is equivalent to the cylindrical charge. Moreover, the total length of the spherical charge pack after superposition should be consistent with that of the columnar charge [23]. The bursting particle expansion loading method is adopted, and the bench blasting simulation is shown in Figure 4.

5. Morphology Comparison of the Muck Pile

The height of the muck pile formed after step blasting and the throwing distance of the rock will directly affect the efficiency of rock cleaning work after blasting [24]. After the blasting test, the parameters of the muck pile formed after the step blasting test were recorded in time to ensure the site's safety. The throwing distance of rocks was determined by a UAV's aerial shot of the blasting area and erected scales

Table 2: Values of microparameters.

Variable parameters	Parameter name	Numerical value
Contact stiffness ratio	Kratio	3.0
Equivalent elastic modulus (GPa)	E*	42
Normal strength of parallel bond (MPa)	Pb_toh	115
Tangential strength of parallel bond (MPa)	Pb_coh	90

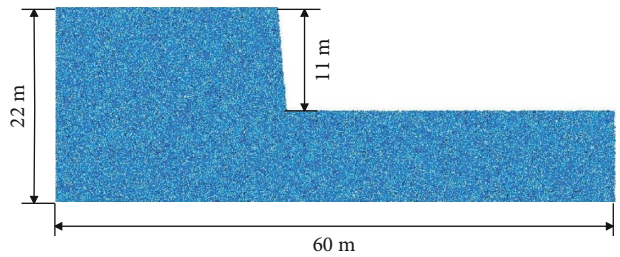

Figure 3: Model diagram of bench blasting.

on the site measured by the height of the muck pile. The aerial shot and the height of the muck pile by UAV are shown in Figures 5 and 6.

After the test, the height of the muck pile measured was 5.53 m and the throwing distance was 42.87 m. According to Figures 5 and 6 on-site, significant chunks appeared in the front of the muck pile, among which the maximum chunk size was 1.32×1.2 m. Analysis of the rock movement process found that the large blocks are mainly generated from the rock mass between the blocked section of the step blast holes and the empty surface of the bench. The rock breakage between the behind row blast holes is relatively sufficient, and the bulk rate is low. The reason is that, after the detonation of the front charge, the stress wave and explosive gas also affect the rock between the behind row blast holes and the rock mass, resulting in cracks in the rock mass. The rocks between the front and behind blast holes will collide with each other to further improve the crushing effect, so the rock breakage is relatively sufficient [25].

The numerical simulation of the blasting heap, as shown in Figure 7, shows that the front of a large piece of rock is more. These chunks come from between the blast holes of the first row of the model, and the bench-free face, especially the hole-plugging section, positions chunks of rock particles to produce more. Simulation of large pieces is greater than that of the actual rock, and the degree of rock simulation error is bigger. The height of the muck pile by numerical simulation is 5.86 m, and the throwing distance is 39.74 m. The simulated height is slightly larger than the actual height, with an error of 5.97%, and the throwing distance is marginally smaller than the real, with an error of 7.88%. The error value is within the acceptable range, indicating that the PFC is feasible and accurate to simulate the form of the muck pile and throwing distance of step blasting [26].

The error between the simulated rock size and the actual situation is significant, and the shape of the blast pile is relatively close to the actual situation. The reason is that the step model is two-dimensional. The model of detonating considered the blasting delay between rows and did not consider the field test existing between the blasting delay between holes. The blasting delay between rows greatly influences the throwing distance of the muck pile, and the blasting delay between holes greatly influences rock fragmentation.

6. Analysis of Influencing Factors of the Open-Pit Bench Blasting Effect

A new bench blasting model is established based on the model parameters verified by field tests. The parameters of deep bench blasting are as follows: the bench height is 5.5 m, the blast hole diameter is 90 mm, the blast hole depth is 6.5 m, the blasting delay between four rows is 30 ms, the spacing of the blast hole row is 2 m, and explosive consumption per unit volume is 0.53 kg/m^3 [27]. The left and lower boundaries of the model are nonreflective, simulating the propagation of infinite media blasting.

6.1. Analysis of the Shape of the Muck Pile with Different Resistance Lines. For the bench blasting simulation, the blasting parameters, such as the charge amount of the blast hole, the blast hole distance, and the extra depth of the blast hole, were kept unchanged. The size of the resistance lines of the first row of blast holes near the free face of the bench was changed, set as 1.0 m, 1.25 m, 1.5 m, 1.75 m, and 2.0 m, respectively. The blasting effect of the different resistance lines was analyzed for bench blasting.

Figure 8 shows the shape of the muck pile when the resistance line is 1.0 m, 1.5 m, 1.5 m, 1.75 m, and 2 m. The statistical situation of the explosive heap height and rock throwing distance is shown in Table 3. It can be seen from Figure 8 that the larger the resistance line, the larger the chunk of rock in the front of the muck pile, and the larger the chunk size, it means that the rock is not broken enough. Large rock blocks appear in the middle and rear of the muck pile, and the main reason is that the row spacing between the behind row blast holes is significant, resulting in insufficient rock fragmentation. The rock blasting area was cut into fragments by longitudinal and transverse cracks, and there are only a few radial tensile cracks in the rock mass to the left of the blast holes of the last row. It indicates that the energy generated by blasting acts mainly on the rock mass on the right side of the blast holes, the rock movement is also along the direction of the minimum resistance line, and the millisecond delay blasting has a particularly protective effect on the retained rock mass.

The height of the muck pile increases gradually with an increase in the resistance line. Moreover, the throwing distance decreases with an increase in the resistance line. The

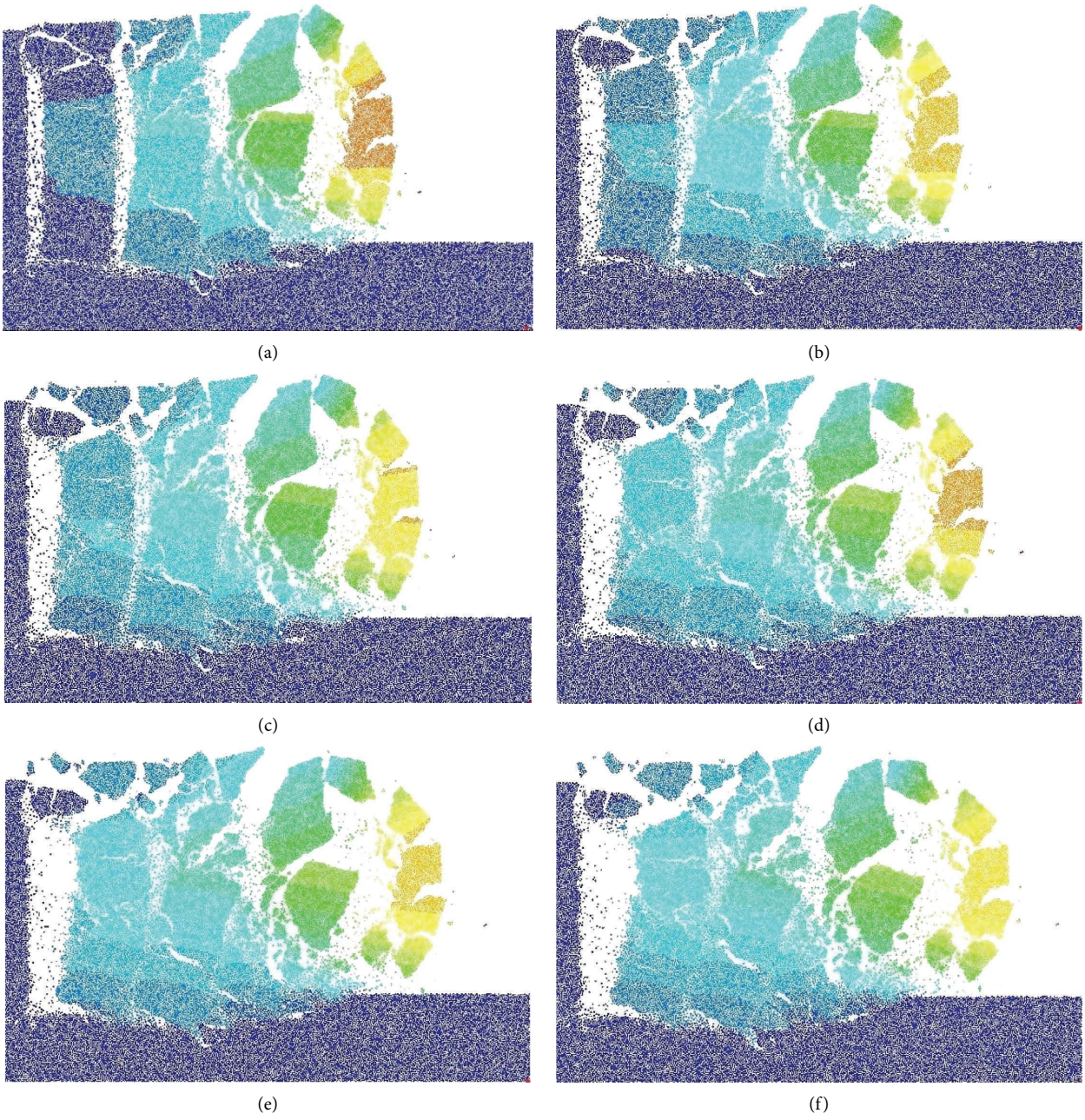

Figure 4: Simulation of the bench blasting process.

Figure 5: Blasting muck pile's height map.

main reasons are as follows: the larger the resistance line is, the larger the volume of rock from the blast holes of the first row to the free face and the larger the volume of rock that

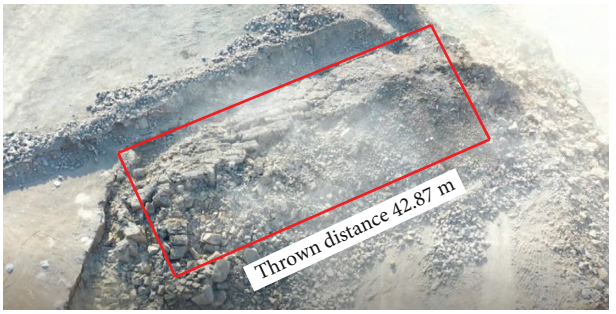

Figure 6: UAV aerial view of the explosion area.

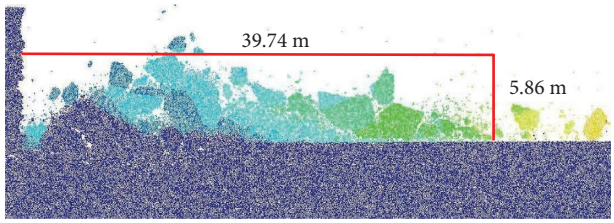

Figure 7: The shape of the simulated blasting.

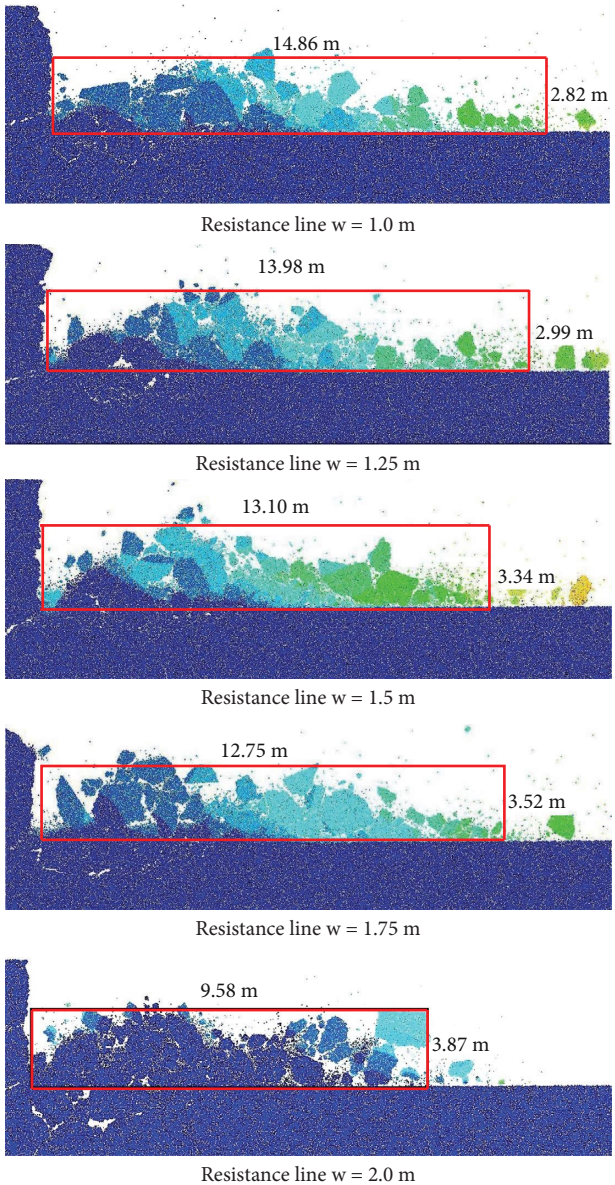

Figure 8: Blasting muck pile's shapes under different resistance lines.

needs to be broken and thrown. The energy generated by the explosion with the same charge is constant, so the blasting energy allocated to unit rock decreases accordingly, resulting in insufficient throwing kinetic energy of rock, reduced throwing distance, and increased muck pile height. As shown in Table 3, when the resistance line increases by 0.25 m, the pile height increases by 6.03%, 11.70%, and 5.38%, respectively. It can be seen from the analysis that the change rate of the height of the muck pile and the throwing distance are increasing-decreasing-increasing and that there is a strong correspondence between the two.

Table 3: Blasting muck pile's sizes under different resistance lines.

Resistance line (m)	Muck pile's height (m)	Thrown distance (m)
1.0	2.82	14.86
1.25	2.99	13.98
1.5	3.34	13.10
1.75	3.52	12.75
2.0	3.87	9.58

Analysis of the relationship between the resistance line w and the rock throwing distance y is carried out, and curve fitting of data points obtained the relationship between the resistance line and the rock throwing distance. The fitting curve is drawn in Figure 9. The correlation coefficient R^2 of the fitting formula is 0.93. When the resistance line is between 1.0 and 2.0 m, the relationship between the throwing distance and the resistance line is shown in formula (4). According to the relationship curve, the relationship between the resistance line and the rock throwing distance is nonlinear and the throwing distance of the rock decreases with an increase in the resistance line. When the resistance line is 1.0 m, the maximum throwing distance of the rock is 14.86 m:

$$y = -4.63w^2 + 9.17w + 10.09. \quad (4)$$

The relationship between the resistance line W and the height of the muck pile z was analyzed. Curve fitting was performed on data to obtain the relationship between the resistance line and the height of the muck pile, and the fitting curve is plotted in Figure 10. The correlation coefficient R^2 of the fitting formula is 0.99. When the resistance line was between 1.0 m and 2.0 m, the relationship between the height of the muck pile and the resistance line is shown in formula (5). It can be seen from the relationship curve that the resistance line and the height of the muck pile are nonlinear and that the height of the muck pile increases with an increase in the resistance line. When the resistance line is 2 m, the maximum height of the pile is 3.87 m:

$$z = 0.22w2 + 0.4w + 2.19. \quad (5)$$

The ratio of the height of the muck pile H to the height of step h is an important index to evaluate the form of the muck pile. Presently, the bench blast casting of sound effects and significant economic benefit is used in engineering blasting at home and abroad, and the value range of H/h adopted by most of them is between 0.6 and 0.9. When the resistance lines are 1.0 m, 1.0 m, 1.5 m, 1.5 m, 1.75 m, and 2 m, the H/h ratios are 0.52, 0.54, 0.61, 0.64, and 0.70, respectively. When the resistance line increases by 0.25 m, the blasting muck pile's height increases by 6.03%, 11.70%, 5.38%, and 9.94%, respectively, and the throwing distance decreases by 5.92%, 6.29, 2.67%, and 24.86%, respectively. When the resistance

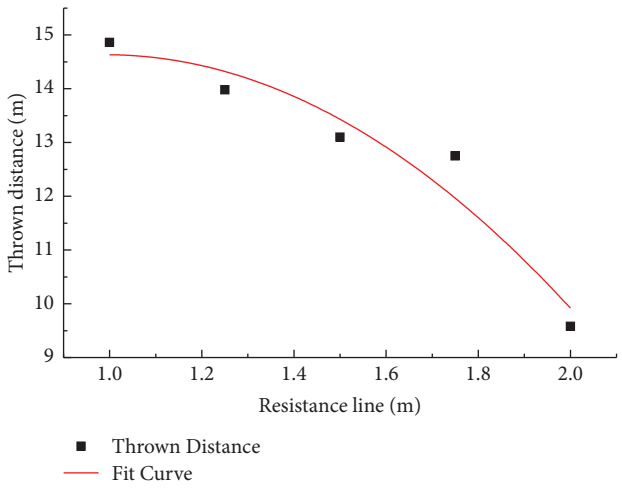

Figure 9: Rock throwing distance relationship curve.

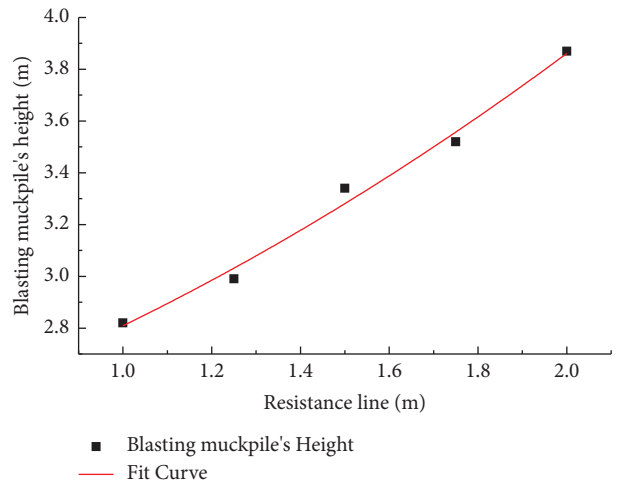

Figure 10: Height of the muck pile relationship curve.

line is 1.75 m, the height of the muck pile increases by only 5.38% and the throwing distance decreases by 2.67% compared with that of 1.5 m. When the resistance line reaches 2 m, compared with 1.75 m, the height of the muck pile increases to 9.94% and the throwing distance decreases to 24.86%. The rocks are stacked together, which is not conducive to subsequent rock loading and transportation. Therefore, when the resistance line is 1.75 m, the ratio of H/h is 0.64, the rock throwing distance decreases moderately, and the rock does not accumulate excessively. At the same time, considering the requirements of the blasting site for throwing distance and blasting muck pile's height, the optimal size of the resistance line of the bench blasting model is 1.75 m.

6.2. Analysis of the Influence of Different Row Delays on the Shape of the Blasting Pile. The reasonableness of the millisecond interval used in blasting will seriously affect rock's blasting quality and vibration effect. Therefore, determining the reasonable blasting delay between rows for blasting

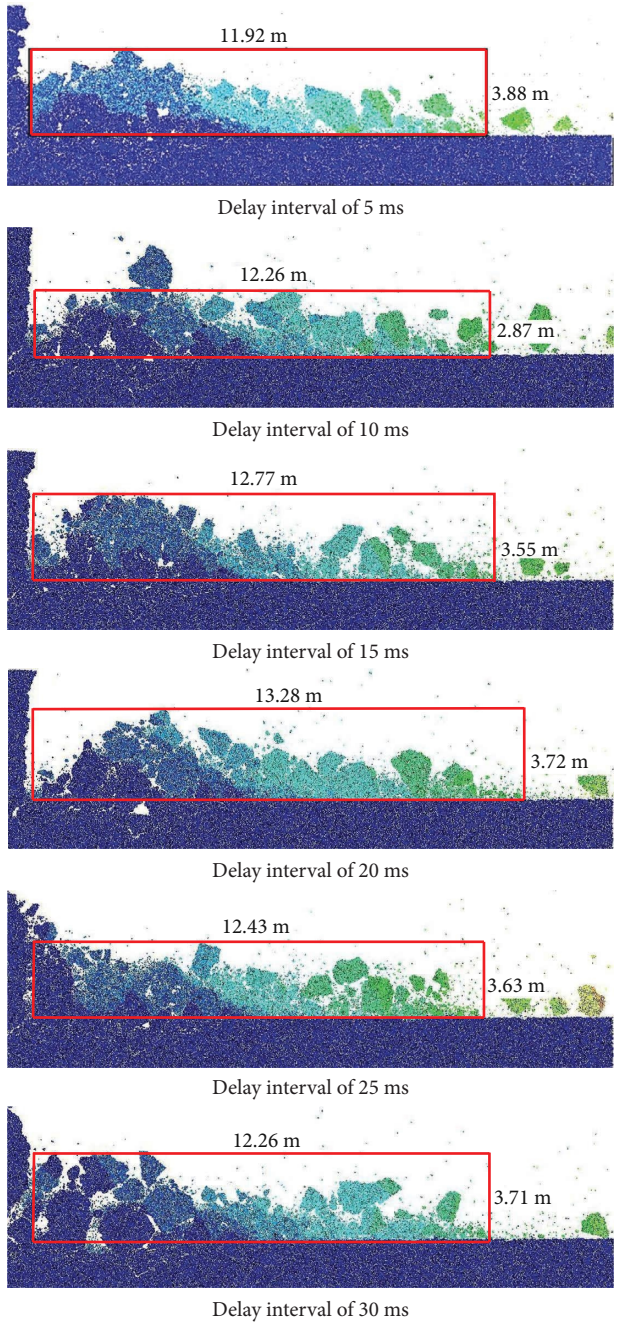

Figure 11: Blasting muck pile's shapes under different delay time difference.

design is significant. Rock properties, hole distance, row spacing, site requirements, and other influencing factors should be considered to determine the delay interval. If the blasting delay between rows is too long, the blasting effect is equivalent to that of the single-hole blasting funnel playing its role one by one, and sometimes it will even affect the blasting network. If the blasting delay between rows is too short, and the new free surface has not been formed when the behind row blast holes are detonated, the millisecond blasting effect cannot be achieved. Therefore, the reasonable blasting delay between rows should be when the previous

row of blast holes forms a free face for the next row of blast holes.

The resistance line of the model was fixed at 1.75 m, the hole distance was 2 m, and the other bench parameters and blasting parameters were consistent with the original model. The blasting delay interval between four rows of blast holes was kept the same, and the blasting delay time between blast holes was changed. Respectively, the delay interval between 5 ms, 10 ms, 15 ms, 20 ms, 25 ms, and 30 ms was used to simulate the model. As shown in Figure 11, the influence of different delay intervals on the muck pile parameters is explored by analyzing the muck pile parameters after blasting. When marking the height and throwing distance of the muck pile, the influence of the occasional large rock on the height and throwing distance of the muck pile is not considered because the occasional large rock will significantly impact the original size of the muck pile. The size marking of the muck pile is mainly based on the height and throwing distance of the overall shape of the muck pile.

Table 4 shows the data statistics of the height of the muck pile and rock throwing distance under different delay intervals. Then, according to the statistical data in Table 4, the point diagram of the size of the muck pile is drawn, as shown in Figure 12. By analyzing the data in the figure, it can be seen that when the resistance line of the front row blast hole is 1.75 m, the height of the muck pile formed is between 2.8 m and 3.9 m and the throwing distance is between 11.9 m and 13.3 m. The overall shape of the muck pile increases with the delay interval and gradually flattens out. The following conclusions can be drawn by analyzing the size data of the muck pile under different delay intervals.

When the delay interval changes between 5 ms and 10 ms, the muck pile's height decreases with the delay interval's increase, which decreases by 26.03%. The reason mainly is the delay interval being too small. After the behind row charge detonated, the front of the rock movement distance was not enough, failing to create a free face for the back rock and impeding the back row of the rock movement. The loose degree of rock between the front and behind blast holes is poor due to excessive extrusion, which leads to increased blasting backlash and the height of the muck pile. When the delay interval is 10 ms, the rock movement in the front row creates a sure free face and rock movement space for the rock movement in the behind row, the hindrance between rocks weakens, and the height of the muck pile decreases.

When the time interval is from 10 ms to 20 ms, the height of the muck pile increases, and the main reason for this phenomenon is the delay interval becoming larger. The movement of the front row rock for the behind row rock movement creates enough free face and space, but the retarding effect on rock movement in the behind row decreases gradually. Meanwhile, jostling each other between rock-broken degrees is abate because the rock mass is bigger, the loose degree is high, and the high of the muck pile begins to become bigger.

When the delay interval changes between 20 ms and 30 ms, the height of the muck pile does not change significantly and the maximum change range is only 2.42%. It can be approximated that the delay interval does not affect the height of the muck pile. As shown in Figure 12, when the delay interval reaches 30 ms, the rate of large rock mass in the muck pile increases significantly. This is because when the delay interval is too large, the collision between the front and back rocks is weakened, and the crushing effect of the rocks is reduced. So this is not conducive to shovel loading and transporting rocks after blasting. Therefore, under the model condition, a delay time of 30 ms is too large to be used.

The rock throwing distance before the delay time increases to 20 ms has been increasing, but the throwing distance decreased after 20 ms. Analysis of the throwing distance's cause decreased, mainly when the delay interval was too big. The front row of rocks stops motion when the throw is complete, and the front row of the rocks hampers the behind row of rock movement to here; thus, throwing distance begins to decrease.

Considering the influence of the delay interval on the height of the muck pile and the throwing distance, when the ratio of the height of the muck pile H to the height of the bench h is controlled between 0.6 and 0.9, the height of the muck pile and the throwing distance of rock should be minimized as much as possible, to reduce the space occupied by the muck pile as much as possible. The loading mechanism has a higher efficiency at shoveling rock. When the delay interval is 25 ms, and the pile height H to bench height h is between 0.6 and 0.9, the blasting muck pile's height and rock throwing distance are relatively small. Therefore, the optimal blasting delay between rows for the bench model is 25 ms.

Table 4: Blasting muck pile's size under different delay intervals.

Delay interval (ms)	Muck pile's height (m)	Thrown distance (m)
5	3.88	11.92
10	2.87	12.26
15	3.55	12.77
20	3.72	13.28
25	3.63	12.43
30	3.71	12.26

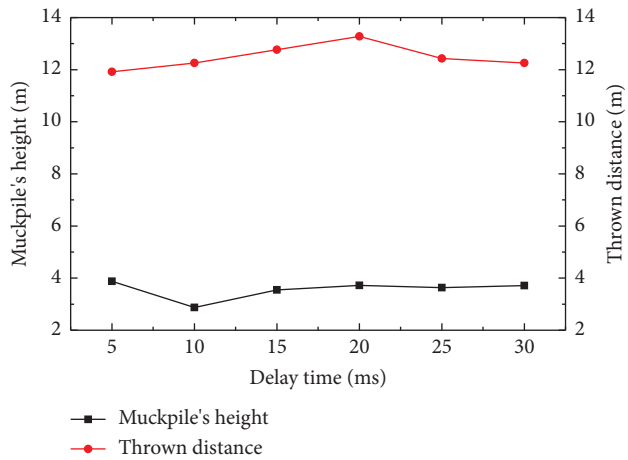

Figure 12: Dot-line diagram of the muck pile's size.

7. Conclusion

By comparing the difference between the simulated result and the result in the muck pile height, the model's rationality is verified and the error value is in an acceptable range. It is feasible to simulate the open-pit bench blasting process with PFC. At the same time, a model is established to optimize the blasting effect by adjusting the resistance line and the delay between the rows.

(1) Adjusting the resistance line size found that the muck pile height is proportional to the resistance line, and the rock throwing distance is inversely proportional to the resistance line. The best resistance line is 1.75 m, according to the effect of the muck pile.

(2) Analyzing the relationship between the resistance line w, the rock throwing distance y, and the blasting muck pile's height z found that the relationship between the resistance line and the throwing distance and the height of the muck pile is nonlinear. The fitting relationship between the resistance line, the rock throwing distance, and the muck pile height was obtained by curve fitting with the data points.

(3) Changing the blasting delay between rows found that when the delay interval changes between 5 and 30 ms, the muck pile height decreases first, then increases, and finally becomes stable. When the delay interval increases to 20 ms, the throwing distance of the rock increases continuously; after 20 ms, the throwing distance decreases. Considering the effect of the delay interval on the height and throwing distance of the muck pile, the optimal blasting delay between rows in the bench blasting model is 25 ms.

Data Availability

The data used to support the findings of this study are available from the corresponding author upon request.

Conflicts of Interest

The authors declare that they have no conflicts of interest.

Acknowledgments

This research was supported by the National Natural Science Foundation of China (inos. 51874189).

References

[1] D. Liu and Z. Wang, "Bulge motion and projectile accumulation," *Explosion and Shock Waves*, no. 03, pp. 1–9, 1983.

[2] C. Liu, M. Y. Yang, H. Y. Han, and W. P. Yue, "Numerical simulation of fracture characteristics of jointed rock masses under blasting load," *Engineering Computations*, vol. 36, no. 6, pp. 1835–1851, 2019.

[3] H. M. An, H. Y. Liu, H. Y. Han, X. Zheng, and X. G. Wang, "Hybrid finite-discrete element modelling of dynamic fracture and resultant fragment casting and muck-piling by rock blast," *Computers and Geotechnics*, vol. 81, pp. 322–345, 2017.

[4] H. M. An, Y. S. Song, H. Y. Liu, and H. Y. Han, "Combined finite-discrete element modelling of dynamic rock fracture and fragmentation during mining production process by blast," *Shock and Vibration*, vol. 2021, Article ID 6622926, 18 pages, 2021.

[5] S. Prasad, B. S. Choudhary, and A. K. Mishra, "Effect of stemming to burden ratio and powder factor on blast induced rock fragmentation-A case study international conference on materials," *Alloys And Experimental Mechanics*, vol. 225, 2021.

[6] T. Hudaverdi and O. Akyildiz, "A new classification approach for prediction of flyrock throw in surface mines," *Bulletin of Engineering Geology and the Environment*, vol. 78, pp. 177–187, 2019.

[7] Z. Yu, X. Z. Shi, Z. X. Zhang, Y. G. Gou, X. H. Miao, and I. Kalipi, "Numerical investigation of blast-induced rock movement characteristics in open-pit bench blasting using bonded-particle method," *Rock Mechanics and Rock Engineering*, vol. 55, no. 6, pp. 3599–3619, 2022.

[8] P. Yan, W. X. Zhou, W. B. Lu, M. Chen, and C. B. Zhou, "Simulation of bench blasting considering fragmentation size distribution," *International Journal of Impact Engineering*, vol. 90, pp. 132–145, 2016.

[9] D. Su, Y. Peng, W. Lu, and M. Chen, "PFC simulation of blast pile morphology in open-air step blasting," *Blasting*, vol. 29, no. 03, pp. 35–41, 2012.

[10] P. P. Procházka, "Application of discrete element methods to fracture mechanics of rock bursts," *Engineering Fracture Mechanics*, vol. 71, no. 4-6, pp. 601–618, 2004.

[11] J. Zhou, Y. Chi, Y. Chi, and J. Xu, "Particle flow method and PFC2D program," *Rock and Soil Mechanics*, no. 03, pp. 271–274, 2000.

[12] J. Yang, C. Shi, W. Yang, X. Chen, and Y. Zhang, "Numerical simulation of column charge explosive in rock masses with particle flow code," *Granular Matter*, vol. 21, no. 4, 2019.

[13] L. Ma, X. P. Lai, J. G. Zhang, S. S. Xiao, L. M. Zhang, and Y. H. Tu, "Blast-casting mechanism and parameter optimization of a benched deep-hole in an opencast coal Mine," *Shock And Vibration*, vol. 2020, Article ID 1396483, 11 pages, 2020.

[14] S. Kim, W. Jeong, D. Jeong, and J. Seok, "Numerical simulation of blasting at tunnel contour hole in jointe rock mass," *Tunnelling and Underground Space Technology*, vol. 21, no. 3-4, pp. 306-307, 2006.

[15] Y. Yang, X. Ding, W. Zhou et al., "Open-pit mine geological model construction and composite rock blasting optimization research," *Shock And Vibration*, vol. 2022, no. 8, Article ID 1468388, 9 pages, 2022.

[16] E. Kabwe, "Velocity of detonation measurement and fragmentation analysis to evaluate blasting efficacy," *Journal of Rock Mechanics and Geotechnical Engineering*, vol. 10, pp. 523–533, 2018.

[17] F. P. Zhang, G. L. Yan, J. Y. Peng, Z. G. Qiu, and X. H. Dai, "Experimental study on crack formation in sandstone during crater blasting under high geological stress," *Bulletin of Engineering Geology and the Environment*, vol. 79, no. 3, pp. 1323–1332, 2020.

[18] Z. Zhang, W. Gao, and K. Li, "Numerical simulation of rock mass blasting using particle flow code and particle expansion loading algorithm," *Simulation Modelling Practice and Theory*, vol. 104, 2020.

[19] H. Hadi, S. Vahab, and F. M. Mohammad, "Static and dynamic response of rock engineering models," *Iranian Journal of Science and Technology, Transactions of Civil Engineering*, pp. 327–341, 2022.

[20] P. Zhang, R. Bai, X. Sun, H. Li, H. Fei, and S. Bao, "A study of millisecond blasting on high bench at barun iron ore operation," *Geofluids*, vol. 2021, Article ID 3645438, 13 pages, 2021.

[21] J. Guo, G. Xu, H. Jing, and T. Kuang, "Fast determination of meso-level mechanical parameters of PFC models," *International Journal of Mining Science and Technology*, vol. 23, no. 1, pp. 157–162, 2013.

[22] J. Shi, X. Miao, H. Meng, H. An, and W. Zhang, "Study on critical damage width of parallel double-free surface blasting," *Frontiers in Earth Science*, vol. 10, Article ID 884558, 2022.

[23] Z. M. Yin, D. S. Wang, X. G. Wang, Z. H. Dang, and W. T. Li, "Optimization and application of spacing parameter for loosening blasting with 24-m-High bench in barun open-pit mine," *SHOCK and vibration*, vol. 2022, Article ID 6670276, 13 pages, 2021.

[24] Y. S. Miao, Y. P. Zhang, D. Wu, K. B. Li, X. R. Yan, and J. Lin, "Rock fragmentation size distribution prediction and blasting parameter optimization based on the muck-pile model," *Mining Metallurgy & Exploration*, vol. 38, no. 2, pp. 1071–1080, 2021.

[25] Z. Zhang, "Kinetic energy and its applications in mining engineering," *International Journal of Mining Science and Technology*, vol. 27, no. 2, pp. 237–244, 2017.

[26] N. K. Bhagat, A. Rana, A. K. Mishra, M. M. Singh, A. Singh, and P. K. Singh, "Prediction of fly-rock during boulder blasting on infrastructure slopes using CART technique," *Geomatics, Natural Hazards and Risk*, vol. 12, no. 1, pp. 1715–1740, 2021.

[27] Y. X. Chen, P. F. Wang, J. Chen, M. Zhou, H. X. Yang, and J. Y. Li, "Calculation of blast hole charge amount based on three-dimensional solid model of blasting rock mass," *Scientific Reports*, vol. 12, no. 1, p. 541, 2022.